OPTIMIZATION AND DESIGN OF THREE-DIMENSIONAL AERODYNAMIC CONFIGURATIONS OF ARBITRARY SHAPE BY A VORTEX LATTICE METHOD

Winfried M. Feifel
The Boeing Company

SUMMARY

A new method based on vortex lattice theory has been developed which can be applied to the combined analysis, induced drag optimization, and aerodynamic design of three-dimensional configurations of arbitrary shape. Geometric and aerodynamic constraints can be imposed on both the optimization and the design process. The method is compared with several known analytical solutions and is applied to several different design and optimization problems, including formation flight and wingtip fins for the Boeing KC-135 tanker airplane. Good agreement has been observed between the theoretical predictions and the wind tunnel test results for the KC-135 modification.

5

INTRODUCTION

Falkner (ref. 1) has used vortex lattice networks as early as 1943 for the calculation of the aerodynamic forces on surfaces of arbitrary shape. With the advent of electronic digital computers, vortex lattice methods were the first powerful tools for three-dimensional potential flow analysis. In the past decade, vortex lattice computer codes were developed independently by several investigators, including Rubbert (ref. 2) and the author of this paper (ref. 3).

The vortex lattice approach is still favored for many engineering applications for several reasons, such as the ease of the problem description, the relatively small computational effort required and the "remarkable accuracy of the solution", as noted by James (ref. 4). One specific advantage of the vortex lattice idealization over the advanced panel methods is that the leading edge suction force is inherently included in the solution. This allows the computation of the configuration induced drag without resorting to the Trefftz-plane theorem.

Vortex lattice methods tend to slightly underpredict induced drag, as observed by Rubbert (ref. 2) and Kalman (ref. 5). However, as long as the paneling scheme is kept uniform, the induced drag computed by the vortex lattice method varies in a consistent fashion from known exact solutions. Therefore, it appears to be justifiable to utilize the vortex lattice near-field induced drag predictions for the optimization of the aerodynamic load distribution.

This paper presents a unified approach for the combined analysis, optimization, and design of three-dimensional aerodynamic configurations based on the vortex lattice technique. The new method will satisfy aerodynamic and geometric constraints while redesigning the contour of the configuration to yield minimum induced drag.

The new combined analysis-optimization-design method takes advantage of the vortex lattice near-field induced drag solution for the optimization process. When linearized boundary conditions with respect to the first guess of the configuration geometry are introduced, the new method can predict with good accuracy the changes in twist and camber required to achieve the load distribution for minimum induced drag and also satisfy additional design constraints.

PROBLEM FORMULATION

A good example of a complex design problem is the addition of wingtip fins to an existing airplane. For a given wing fin height and planform, the task is to determine the fin twist and camber, and the angle of attack of both the fin and the wing that will result in minimal induced drag for the airplane at a prescribed lift coefficient. To accomplish this, a mixed analysis/design problem must be solved. The problem can be stated as follows: Determine the twist and/or camber distribution required for portions or all of a three-dimensional system of wings with arbitrary planforms while a number of prescribed design requirements are satisfied. The design requirements could be any meaningful combination of the condition that the induced drag of the system (or of part of the system) be a minimum while at the same time a number of constraint conditions are imposed. Typical constraints would be, for example, that a given amount of lift be generated at a given pitching or rolling moment, or that the boundary conditions be satisfied on portions of the initial configuration.

Translated into the language of mathematics, the task described above amounts to finding the extremum of a function subject to a set of imposed constraints. Such a problem can be solved by Lagrange's method of multipliers.

SOLUTION

The configuration to be analyzed or designed is subdivided into a network of n panels spaced uniformly in spanwise and chordwise direction, as outlined in figure 1. Based on the theorem of Pistolesi (ref. 6) an unknown lifting vortex singularity γ is located along the 1/4-chord line of each panel. Helmoltz' law is satisfied by shedding a pair of trailing vortices along the panel edges downstream to infinity. It is a basic assumption for this horseshoe vortex model that these trailing vortices are aligned with the local flow direction; therefore, only the forces acting on the lifting vortex elements need to be computed. There are two points of special significance located on each panel: the lifting vortex midpoint and a boundary point at 3/4-chord.

Boundary Conditions

In the configuration analysis mode, the strength of the unknown singularities γ is determined such that the flow tangency condition is satisfied at all boundary points. In the configuration design mode, the boundary conditions need not necessarily be satisfied on the initial geometry, but there the angle formed between the panel surface and the velocity vector at the panel 3/4-chord point represents the unknown values $\Delta\alpha$, $\Delta\beta$ of the changes in panel orientation, which are necessary to yield the contour of the updated configuration.

The boundary condition for the panel j can be written in the generalized form

$$C(\gamma_1, \gamma_2 \ldots \gamma_n, \Delta\alpha_j, \Delta\beta_j) = \sum_{i=1}^{n} \gamma_i f_{ji} - \Delta\alpha_j a_j - \Delta\beta_j b_j - \vec{N}_j \cdot \vec{u}_\infty = 0 \qquad (1)$$

where

f_{ji} = boundary point influence coefficient indicating the velocity induced by a unit strength singularity i parallel to the surface normal vector $\vec{N}_j$ on panel j.

$\Delta\alpha_j, \Delta\beta_j$ = unknown pitch and yaw angles that may be required to reorient the panel j in order to satisfy the flow tangency at its boundary point.

a_j, b_j = panel reorientation influence coefficients that indicate the change in $\vec{N}_j \cdot \vec{u}_\infty$ when the panel j is pitched or yawed by $\Delta\alpha=\Delta\beta=1^o$.

$\vec{u}_\infty$ = free stream velocity vector.

The panel reorientation influence coefficients are linearized with respect to the initial panel location. Therefore equation (1) can be considered accurate for orientation changes of approximately up to $\Delta\alpha_j=\Delta\beta_j=20^o$. If the boundary condition has to be satisfied at the original position of the panel (analysis mode) then $\Delta\alpha_j$ and $\Delta\beta_j$ are zero.

Computation of Forces

The conditions at the 1/4-chord point (vortex midpoint) govern the forces acting on the panel. The velocity vector $\vec{v}_j$ at the 1/4-chord point is obtained as the sum of the free stream velocity vector $\vec{u}_\infty$ and the velocity induced according to Biot-Savert's law by all unknown vortex singularities in the flow field:

$$\vec{v}_j = \vec{u}_\infty + \sum_{i=1}^{n} \vec{w}_{ji} \gamma_i \qquad (2)$$

where $\vec{w}_{ji}$ denotes the velocity induced at the midpoint of panel j by the unit strength horseshoe vortex of panel i. The velocity at the midpoint is assumed to represent the average value over the panel and is used to determine the force $\vec{F}_j$ acting on the panel by applying Kutta-Joukowsky's law for a fluid of unit density:

$$\vec{F}_j = \vec{v}_j \cdot \vec{S}_j \gamma_j \qquad (3)$$

where $\vec{S}_j$ describes the length and orientation of the lifting vortex element.

The force vector $\vec{F}_j$ comprises the panel drag component D_j and the lift vector $\vec{L}_j$, which by definition is oriented normal to the free stream vector $\vec{u}_\infty$.

The induced drag of a whole configuration with n panels can be expressed as a quadratic function of all the panel vortex strengths γ in the form of the double sum:

$$D(\gamma_1 \cdots \gamma_n) = \sum_{j=1}^{n} \gamma_j \sum_{i=1}^{n} d_{ji} \gamma_j \qquad (4)$$

The induced drag influence coefficients d_{ji} describe the drag force experienced by the panel j due to the panel i when their horseshoe vortices have unit strength. The drag influence coefficients contain only geometrical terms. In order to get a nontrivial minimum induced drag solution, at least one constraint must be introduced in addition to equation (4).

Constraint Conditions

There are a large number of different constraint conditions which can be imposed on the minimum induced drag problem. In the present method, any meaningful combination of the following constraints may be specified:

1) Boundary conditions: For each boundary condition to be satisfied, a new equation (1) is introduced.

2) Relationships between unknown singularities: The strength of certain horseshoe vortices or a relationship between groups of horseshoe vortices is introduced via an equation of the type:

$$C(\gamma_1, \gamma_2 \cdots \gamma_n) = \sum_{i=1}^{n} g_i \gamma_i + g_{n+1} = 0 \qquad (5)$$

where the constants (g) are weighting functions describing the particular constraint condition.

3) Relationships between the panel reorientation parameters: The movements of panels or of groups of panels are controlled by the following constraint equations that establish relationships between the unknowns $\Delta\alpha$ and/or $\Delta\beta$:

$$C(\Delta\alpha_1 \cdots \Delta\alpha_n, \Delta\beta_1 \cdots \Delta\beta_n) = \sum_{i=1}^{n} g_i \Delta\alpha_i + \sum_{i=1}^{n} g_{n+1} \Delta\beta_i + g_{2n+1} = 0 \qquad (6)$$

4) Force or moment relationships between groups of panels: Forces and moments due to individual panels or groups of panels are prescribed by equations of the following type:

$$C(\gamma_1, \cdots \gamma_n) = \sum_{i=1}^{n} g_i h_i \gamma_i + g_{n+1} \qquad (7)$$

where the influence coefficient h_i indicates the force or the moment of the panel i for $\gamma_i = 1$.

The influence coefficients h_i are, in principle, described by equation (3). Equation (2) shows that for the computation of h_i, all vortex strengths γ need to be known. Equation (7) therefore is nonlinear. However, rather than solving the nonlinear problem directly, an iterative scheme is employed where the first solution of the vorticity distribution is found for $h_i^{(0)}=h_i(\vec{u}_\infty)$. Subsequent iterations use updated coefficients, $h_i^{(k)} = h_i(\vec{u}_\infty, \gamma_1^{(k-1)},\ldots\gamma_n^{(k-1)})$ which are based on the vortex distribution of the previous solution. This process converges very rapidly, and in many cases the first solution is already sufficiently accurate.

Drag Minimization Under Constraint Conditions

The induced drag function (4) and the constraints C given by the expressions (1) and (5) through (7) may be combined in a new quadratic function:

$$G(\gamma_1\cdots\gamma_n,\Delta\alpha_1\cdots\Delta\alpha_n,\Delta\beta_1\cdots\Delta\beta_n,\lambda_1\cdots\lambda_m)=D(\gamma_1\cdots\gamma_n)+\sum_{i=1}^{m}\lambda_i\,C_i \qquad (8)$$

where λ_i are the Lagrangian multipliers for m constraints imposed. A necessary requirement for the induced drag to be a minimum is that all the partial derivatives of equation (8) be zero. Differentiating the function G with respect to all its variables γ_1 through λ_m yields a system of simultaneous linear equations for the unknowns γ, $\Delta\alpha$, $\Delta\beta$, λ. Solution of this system of equations completes the configuration analysis-optimization-design process, unless an iteration is required to update the influence coefficients h of equation (7) or if the redesigned geometry deviates too much from the starting configuration.

VALIDATION OF THE TECHNIQUE

The vortex lattice analysis-optimization-design method has been programmed in FORTRAN IV on the CDC6600 computer. A series of data cases have been run to check the method against known analytical solutions.

Planar Wings

R. T. Jones (ref. 7) has given an analytical solution for the load distribution about wings of varying spans having the same prescribed lift and wing root bending moment. Some of his cases have been analysed by the present vortex lattice method using a single lifting line subdivided into 40 equal panels. The wingtip panel and its trailing vortex were inset by 1/4-panel span as proposed by Rubbert (ref. 2). The agreement between the vortex

lattice results and Jones' exact solution is excellent for both the shape and the spanwise load distribution (see figure 2) and the induced drag ratios shown in figure 3.

Nonplanar Configurations

Lundry (ref. 8) gives the induced drag factor, e, and the optimum spanwise circulation distribution obtained by a Trefftz-plane analysis of wings with a wingtip mounted end plate. Figure 4 shows the optimum circulation distribution on a wing with a 20% end plate compared to two vortex lattice results obtained with a single lifting line but using a different number of spanwise panels. The agreement with the exact solution is excellent, except in the corner between the wing and the tip fin. There the vortex lattice solution obtained with 25 panels per half-wing deviates slightly from the exact solution.

Some understanding of the source of the slight differences in span loading can be gained by comparing the downwash and sidewash computed at the midpoints of the lifting vortex elements with the known exact distribution. The Trefftz-plane analysis yields constant downwash along the span of the wing and zero sidewash along the span of the tip fin for the minimum induced drag load distribution. The present vortex lattice solution yields essentially the same results, but there are noticeable discrepancies in a small region of the wing-fin intersection, as shown in figure 5. This indicates that under certain conditions, the point selected for induced drag computation should not always be located exactly in the middle of each panel lifting vortex element. This error is, however, confined to a relatively small portion of the configuration and some of the downwash deviations are of oscillatory nature and therefore self-cancelling. The induced drag efficiency factors indicated by the vortex lattice method and by the exact solution are thus practically identical for this particular configuration, as shown in figure 6.

APPLICATION OF THE PRESENT VORTEX LATTICE DESIGN METHOD

The present method has been applied to a variety of problems, such as the design of wingtip fins, the modification of wings of a hydrofoil boat, and the optimum positioning of the leading-edge devices of the YC-14 military transport. The following two examples demonstrate some of the capabilities of the combined analysis-optimization-design vortex lattice method.

Formation Flight

Formation flying techniques have been proposed repeatedly as a means of reducing airplane drag. To get an estimate of the possible savings in induced drag, a group of five airplanes flying at the same altitude in an arrow formation illustrated in figure 7 were analyzed. The ideal (elliptic) load distribution, which yields minimum drag for the whole formation, is well known from the Trefftz-plane analysis. This optimum solution is, however, not practical since none of the airplanes off the centerline would be balanced in roll. In addition, a completely impractical wing twist distribution would be required to achieve such a load distribution. The induced drag savings indicated by this simple theory are, therefore, far too optimistic.

A more realistic picture is obtained by introducing the constraint that each airplane of the formation be trimmed in pitch and roll with respect to its own center of gravity. For this analysis, the airplanes are assumed to have swept, constant chord wings without wing twist. The left-hand and right-hand ailerons of each airplane are interconnected such that they deflect by equal but opposite angles. The horizontal tail is a simple flat plate. The unknown geometry variables are the angular deflections of every surface in the formation; ie, wing and horizontal tail incidences and aileron deflection angles. A lift coefficient of $C_L = 0.5$ is prescribed for the formation.

When only the lift for the whole airplane formation is prescribed, each of the airplanes carries a different amount of load, as seen in the top of figure 8. This distribution of the load between airplanes creates the minimum amount of induced drag for the whole formation flying at the conditions stated.

A more practical result is obtained when the constraint is introduced that each airplane in the formation flies at the same lift coefficient. Then the problem is fully defined, and only an analysis-design scheme has to be implemented. The load distribution and the induced drag values for the airplanes operating under this condition are shown in the center of figure 8.

As a third variant of the formation flight problem, the induced drag of only the No. 2 and No. 4 airplane has been minimized by allowing a redistribution of the formation weight among the other airplanes. The results are shown at the bottom of figure 8. The lift of the No. 2 and No. 4 airplanes is close to zero for minimum induced drag; the small residual lift stems from the condition that the planes are trimmed. This solution is only of academic interest, but it demonstrates the capability of the present method to minimize the induced drag of subsets of a configuration.

The analysis of this five-airplane formation using the vortex lattice method indicates that drag savings can be significant though much smaller than predicted by the idealizing Trefftz-plane assumptions. In addition, it is seen that the induced drag is unevenly distributed among the airplanes in the formation. Therefore, different formation arrangements should be used to obtain a more uniform drag level for all airplanes involved.

Wingtip Fins for the KC-135 Airplane

The present vortex lattice method has been used extensively by Ishimitsu, et al., (ref. 9) to evaluate and design tip fins for the KC-135 tanker airplane.

Figure 9 shows a typical vortex lattice representation of the KC-135 wing with the tip fins. Since the prime area of interest of this study was the region near the wingtip, the body of the airplane was not modeled in potential flow. The small loss in accuracy was believed to be outweighed by the savings in computer time. After a series of trades varying tip fin height and cant angle, the final planform was selected for the tip fin. For this given fin planform, the fin incidence angle and the profile camber shape were designed to yield minimum induced drag, while at the same time the boundary conditions were satisfied on the remainder of the airplane. As a first guess, the wing fin was input as a flat plate. The chordwise vorticity distribution on the fin was approximated by 10 lifting vortex elements, while 6 panels were used in the spanwise direction. Since the induced drag is independent of the shape of the chordwise load distribution (Munck's stagger theorem), the induced drag minimization problem is not fully defined unless a weighting function is introduced that prescribes how the vorticity is distributed among the 10 chordwise lifting elements. The vortex lattice program solves for the optimum total amount of lift carried by each chordwise column and for the orientation of the panels necessary to produce the prescribed chordwise load variation. The airfoil section camber line is obtained by integrating the panel slope changes calculated by the vortex lattice program. Thin airfoil theory has been used to superimpose a suitable thickness distribution and the fin camber lines. The results of this process are shown in figure 10.

The final tip fin configuration was tested in a wind tunnel. Figure 11 shows good agreement between the measured changes in a airplane drag and the predictions of the vortex lattice analysis. The experimental and theoretical loads on the wing and the tip fin are compared in figure 12. Considering that the incompressible vortex lattice analysis did not include the effects of the body and wing thickness, the agreement with the experiment is surprisingly good.

CONCLUSION

The vortex lattice method has been successfully applied to the design and optimization of three-dimensional configurations. The nonlinear analysis-design-optimization problem in which both the geometry or portions thereof and the optimum load distribution are unknown can be solved in a straightforward manner. The validity of the method has been demonstrated by application to several problems, previously not directly amenable to theoretical analysis. The new method has no serious drawbacks, but it must be applied with caution in regions of sudden geometric changes, such as intersecting wing surfaces, in which case additional work is required to determine the best paneling scheme and optimum location of the control points. Even though more advanced panel methods have been developed, the vortex lattice approach is still preferred in many applications for several reasons. The theory is simple and can be translated into fast numerical schemes. The vortex lattice approach, unlike many other methods, accounts for the leading edge suction force and therefore, yields an accurate near-field drag solution. These characteristics make the vortex lattice scheme a powerful tool in the hands of an experienced aerodynamicist for the analysis, modification, and optimization of three-dimensional configurations.

APPENDIX

SYMBOLS

A	Wing area
AR	Wing aspect ratio
b	Wing span
C	Local chord length
$\bar{C}$	Mean chord length
C_D	Total airplane drag
C_{D_i}	Airplane induced drag
$C_{D_{i_{ell}}}$	Induced drag of elliptically loaded wing
C_L	Wing lift coefficient
C_ℓ	Local lift coefficient
e	Induced drag efficiency factor
h	Height of winglet
M_∞	Free stream Mach number
n	Number of panels
S	Wing half span
S_{ell}	Half span of elliptic wing
W	Downwash or sidewash at vortex midpoint
X,Y,Z	Cartesian coordinates
γ	Local vortex strength
η	Nondimensional spanwise station

REFERENCES

1. Falkner, V. M., "The Calculation of Aerodynamic Loading on Surfaces of Any Shape," R&M 1910, 1943, British Aeronautical Research Council.

2. Rubbert, P. E., "Theoretical Characteristics of Arbitrary Wings by a Nonplanar Vortex Lattice Method," Rept. D6-9244, 1964, The Boeing Company, Seattle, Wash.

3. Feifel, W. M., Fortran IV - Programm zur Berechnung von V-Leitwerken," Mitteilung im Institut für Aerodynamik und Gasdynamik der Technischen Universität, Stuttgart, Germany, 1966.

4. James, R. M., "On the Remarkable Accuracy of the Vortex-Lattice Discretization in Thin Wing Theory," Rept DAC-67211, McDonnell Douglas Corp, Long Beach, Calif., Feb. 1969.

5. Kalman, T. P., Giesing, J. P., Rodden, W. P., "Spanwise Distribution of Induced Drag in Subsonic Flow by the Vortex Lattice Method," J. Aircraft, Vol. 7, No. 6, 1970.

6. Pistolesi, E., "Betrachtungen über die gegenseitige Beeinflussung von Tragflügelsystemen." Gesammelte Vortrage der Hauptversammlung 1937 der Lilienthal-Gesellschaft (1937), S. 214-219.

7. Jones, R. T., "The Spanwise Distribution of Lift for Minimum Induced Drag or Wings Having a Given Lift and a Given Bending Moment," NACA Technical Note 2249, Ames Aeronautical Laboratory, Moffett Field, Calif., Dec. 1950.

8. Lundry, J. L., "A Numerical Solution for the Minimum Induced Drag, and the Corresponding Loading, of Nonplanar Wings," NASA CR-1218, issued by originator as Report DAC-66900, McDonnell Douglas Corp., Long Beach, Calif., 1968.

9. Ishimitsu, K. K., Van Devender, N., Dodson, R., "Design and Analysis of Winglets for Military Aircraft," Air Force Wright Aeronautical Laboratories, Wright-Patterson AFB, Ohio, Rpt No. AFFDL-TR-76-6, 1976.

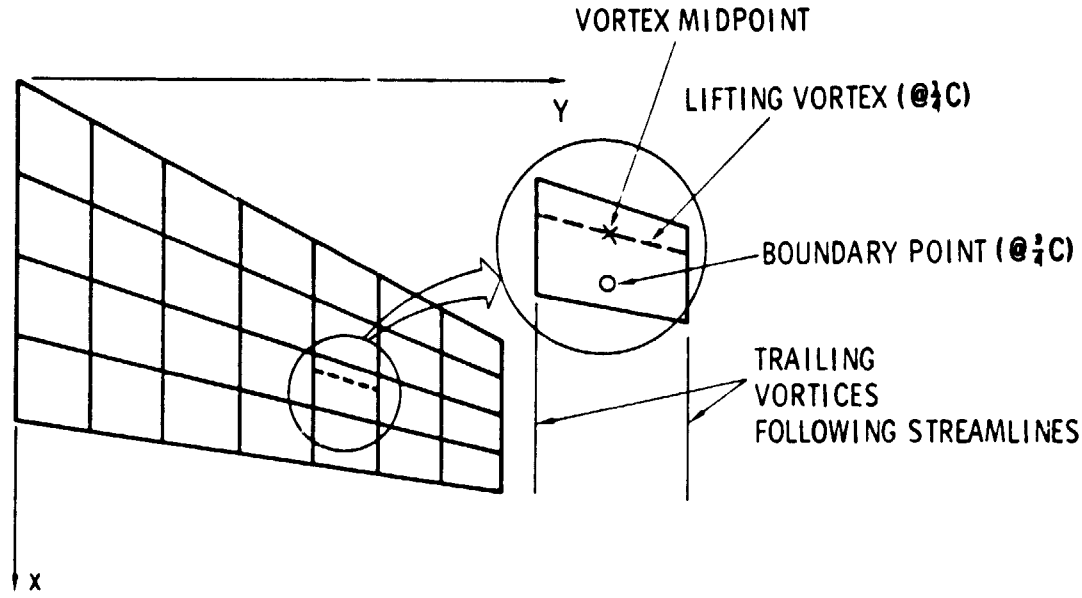

Figure 1.- Surface division into panels and location of vortices and control points.

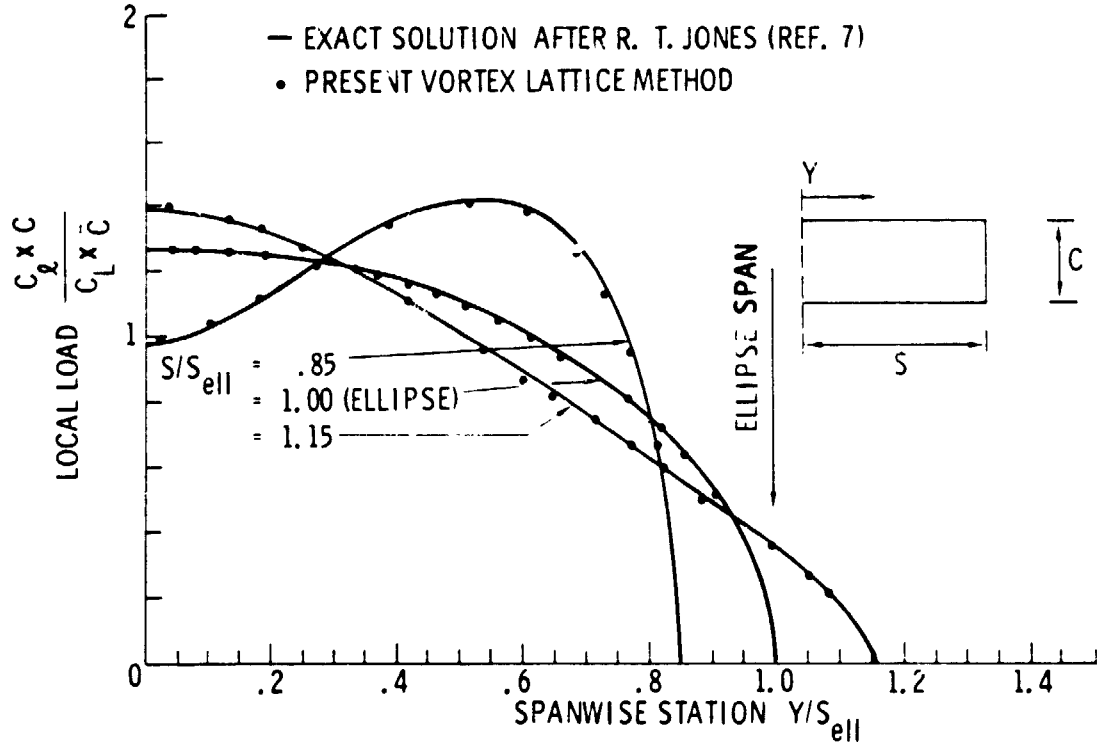

Figure 2.- Spanwise loading curve for minimum induced drag of wings having a fixed total lift and a fixed root bending moment.

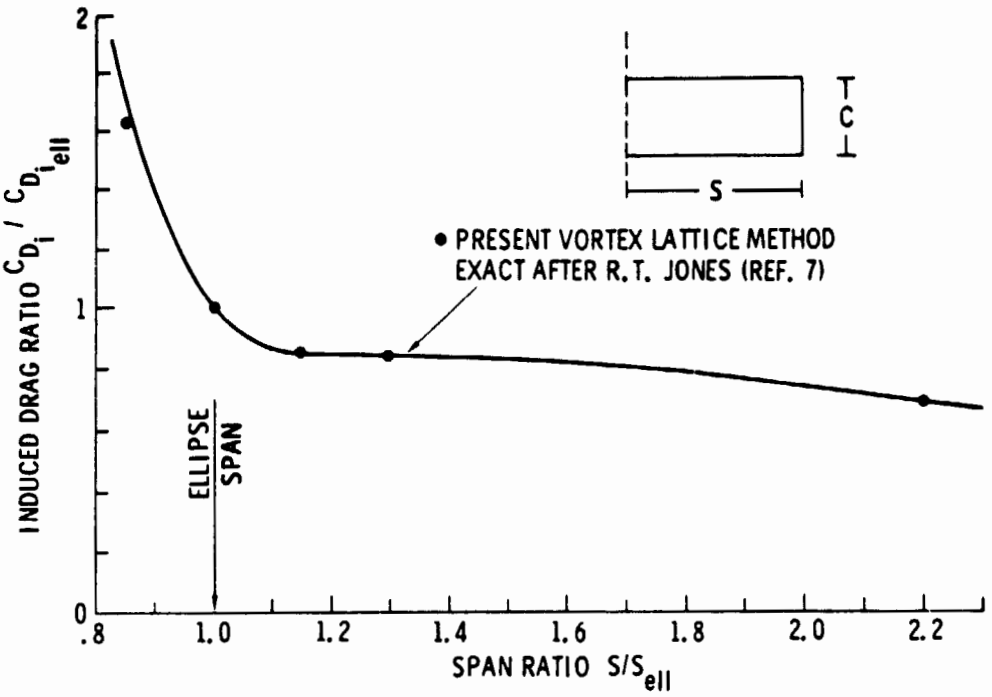

Figure 3.- Variation of minimum induced drag with span for wings having a fixed total lift and a fixed root bending moment.

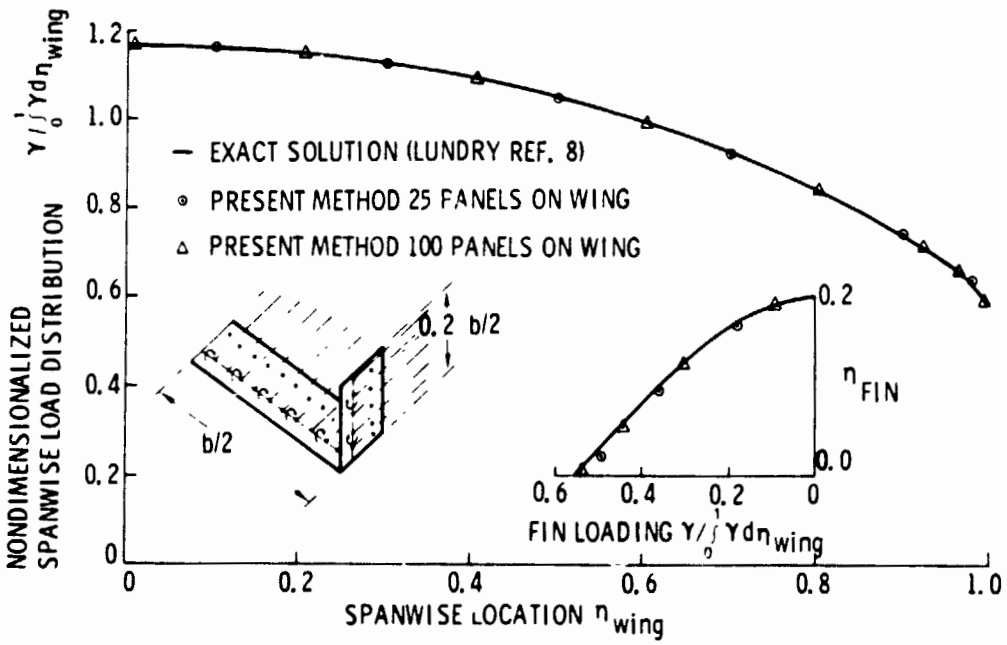

Figure 4.- Optimum load distribution about a wing with an end plate.

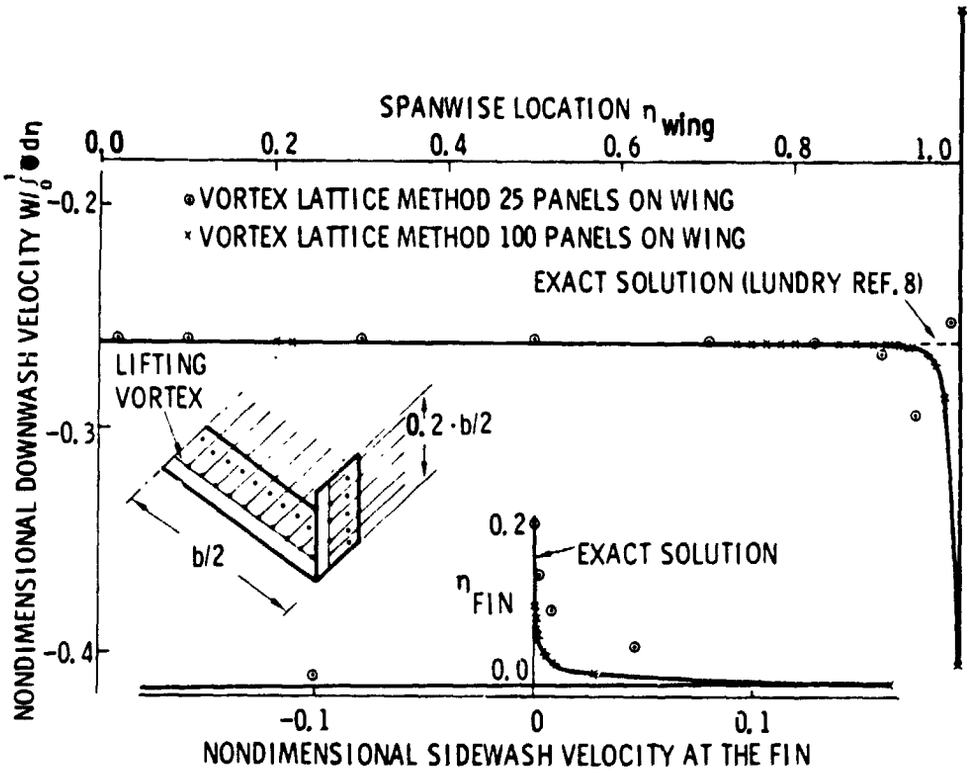

Figure 5.- Downwash and sidewash along the 1/4-chord line of a wing and end plate for the minimum induced drag load distribution.

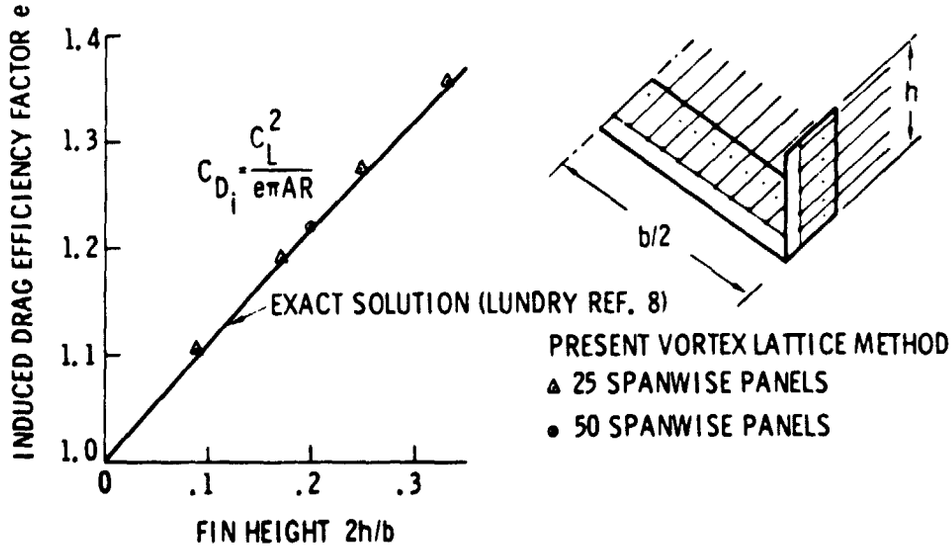

Figure 6.- Induced drag efficiency factor of wings with an end plate.

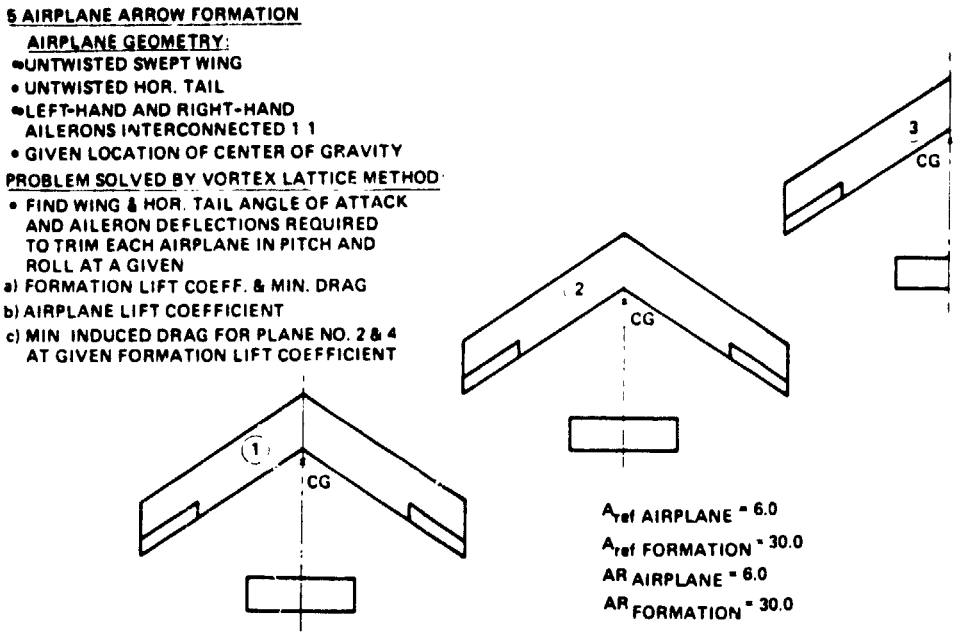

Figure 7.- Five-airplane arrow formation.

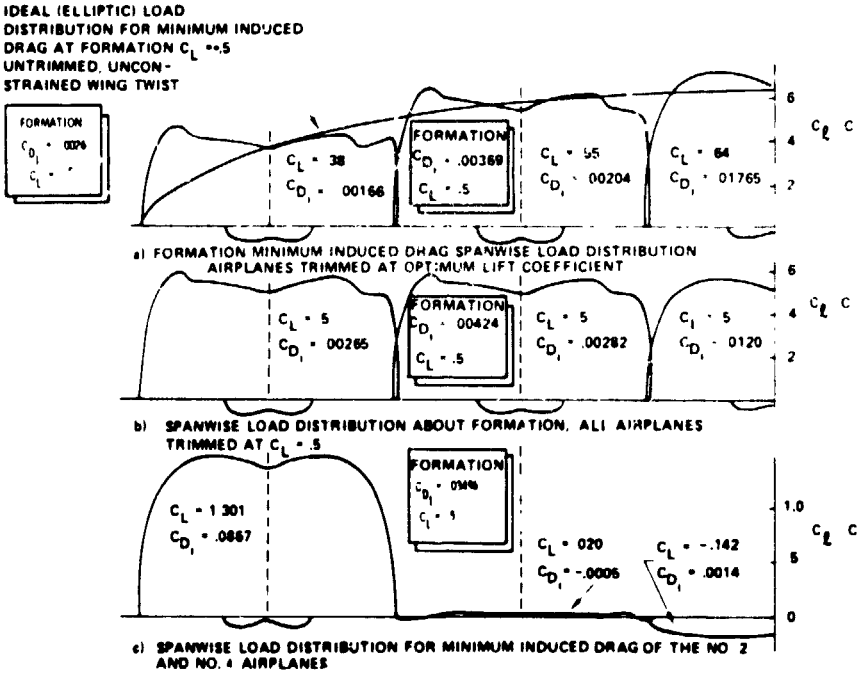

Figure 8.- Spanwise load distributions about five airplanes flying in arrow formation at the same altitude.

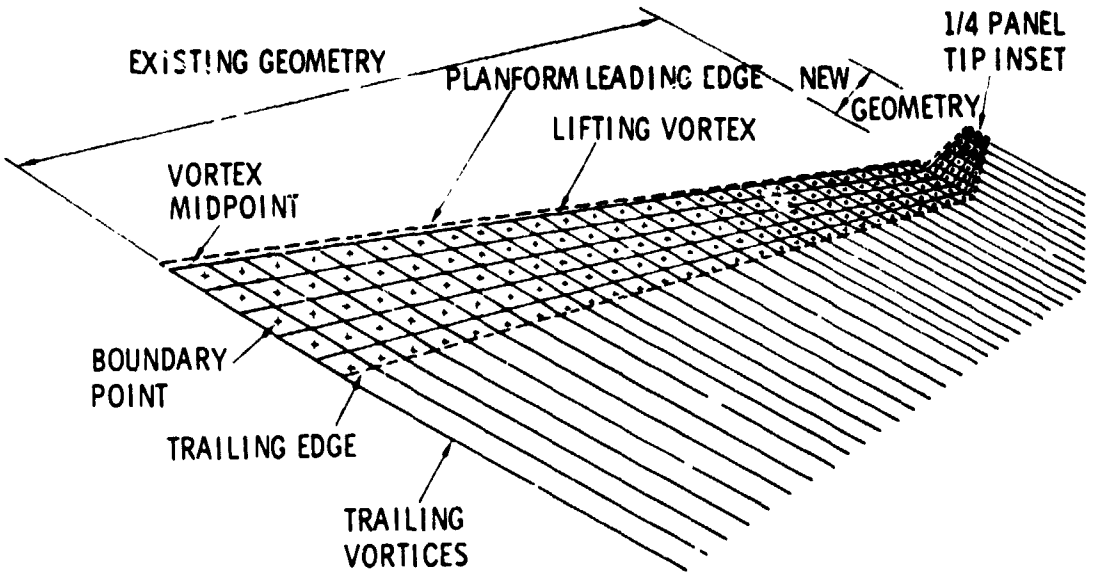

Figure 9.- Typical representation of wing and winglet by a multi-horseshoe vortex lattice system.

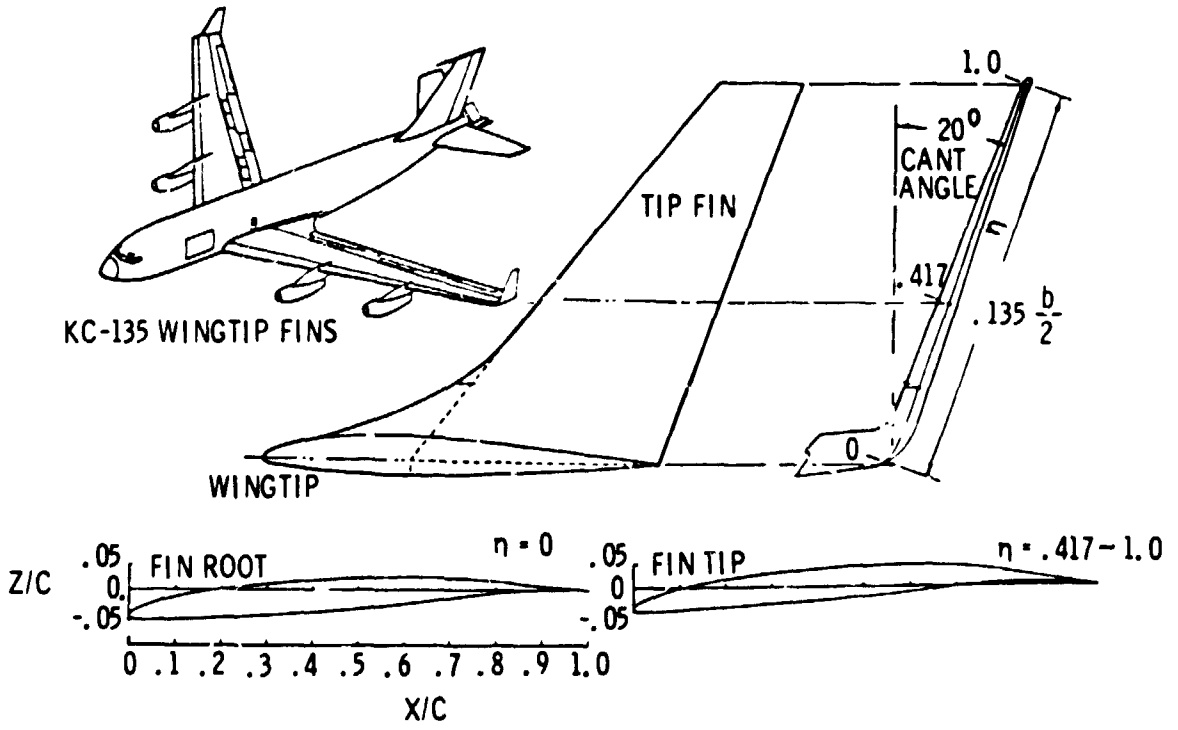

Figure 10.- Tip fin airfoil sections with camber line designed by vortex lattice optimizing method.

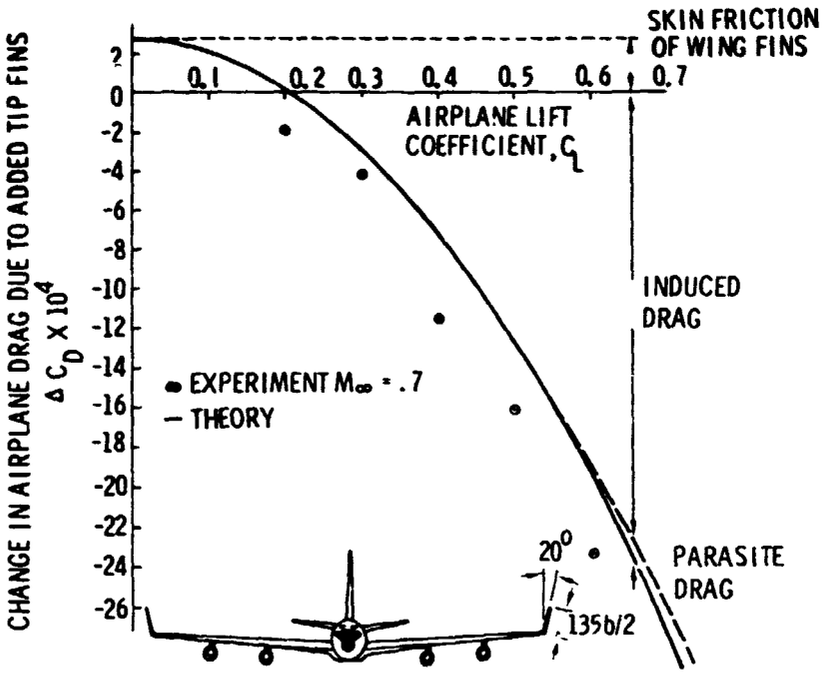

Figure 11.- Measured and predicted drag change of Boeing KC-135 with tip fins.

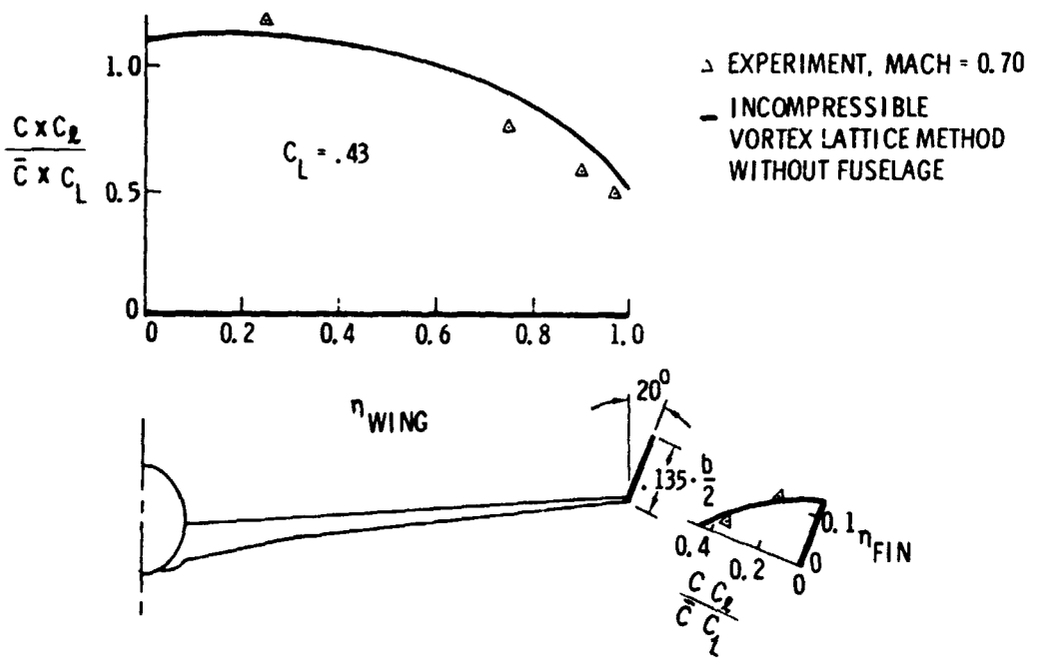

Figure 12.- Comparison between experimental and theoretical span load distribution about KC-135 with tip fins.